On the RMF Impact on the Structure of Solidifying Ingots

B Mikhailovich, A Kapusta, S Khripchenko, S Denisov, V Dolgikh, A Pavlinov

On the RMF Impact on the Structure of Solidifying Ingots

B. Mikhailovich [1], A. Kapusta [1], S. Khripchenko [2], S. Denisov [2], V. Dolgikh [2], A. Pavlinov [2]

[1]Department of Mechanical Engineering,
Ben-Gurion University of the Negev, P.O.B. 653, Beer-Sheva 8410501, Israel
[2]Laboratory of Hydrodynamics, Institute of Continuous Media Mechanics
Korolev 1, Perm 614013, Russia

Corresponding author: borismic@bgu.ac.il

Abstract
We consider the possibility of establishing a relation between the structure of an ingot solidified in a rotating magnetic field and the parameters characterizing magnetohydrodynamic effects. We also report the results of calculations carried out to determine the velocity of melt flow and to evaluate its stability and analyze the characteristics of boundary layers and the velocity of the crystallization front using the experimental data.

Key words: liquid metal flow, cylindrical vessel, rotating magnetic field, "external" friction model, boundary layers, solidification rate, experimental data.

Introduction

Electromagnetic stirring is widely used in metallurgy and foundry for melt homogenization. It also significantly improves the structure and mechanical properties of ingots and cast products. Over a period of years, devices that generate rotating magnetic fields (RMF) are in most common use, because they have simple design and are able to operate together with industrial frequency convertors. However, despite long experience in this field, a choice of optimal values for parameters that characterize magnetohydrodynamic (MHD) effects still remains a complex problem.

There are almost no theoretical and semiempirical mathematical models that relate the ingot structure (size and configuration of macrograins) and the MHD parameters of the melt in the vicinity of the crystallization front. This can probably be attributed to a huge difference in scales used to describe melt flows in terms of a continuum model and ingot structure formation in terms of solid-state physics models.

In order to solve this urgent problem, we have developed a model, where the ingot structure is considered relative to the parameters of the rotating magnetic field, by performing theoretical and experimental assessment of the thickness of a hydrodynamic boundary layer. At the same time, we have examined the appropriate solidification conditions (melt overheating temperature, heat generation intensity and direction and some others) and the corresponding values for RMF parameters. These estimates allowed us to calculate the thickness of a boundary layer and a heat flow passing through this layer.

Problem statement

At the first stage of the problem solving, we consider a 3D melt flow in a rotating magnetic field in experimental conditions simulated in our study [1]-[3].

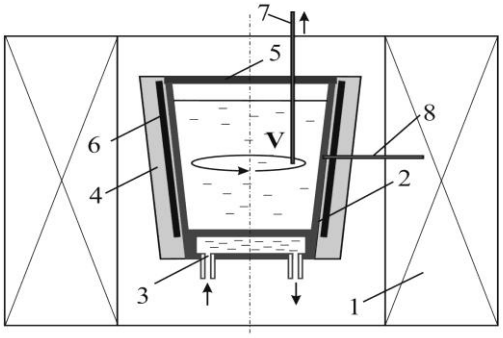

Fig. 1: Scheme of the experimental setup:
1 - MHD stirrer, 2 - mold, 3 - water condenser, 4, 5 - insulated wall and lid, 6 - wall heater, 7 - movable and 8 -fixed thermocouples measuring melt and wall temperatures.

A crucible with liquid metal is a cone-shaped vessel with thin stainless steel sidewalls heated by an electrical heater (Fig. 1). The bottom of the crucible is cooled by water with temperature control. The crucible walls are painted with a special paint to prevent their failure. The average crucible diameter is 126 mm, and the height of a melt column in the crucible reaches 140 mm. In our experiments, tin and aluminum are subjected to directional

solidification in the presence of MHD stirring. Measurements of temperature distribution along the column of liquid metal in the crucible and the position of a solid phase front versus the solidification time are made with a thermocouple probe.

The turbulent MHD flow in a cylindrical mold of an equivalent volume is described in a cylindrical coordinate system (r,φ,z) in non-inductive approximation in terms of an "external" friction model [4] by the following system of equations:

$$\Delta V_\varphi - \lambda V_\varphi = -Ha^2 (r - V_\varphi) K_a , \tag{1}$$

where $\Delta = \frac{\partial^2}{\partial r^2} + \frac{1}{r}\frac{\partial}{\partial r} - \frac{1}{r^2} + \frac{1}{\delta_z^2}\frac{\partial^2}{\partial z^2}$, $\lambda = C_0 \operatorname{Re}_\omega \Omega_z / \delta_z$, $\operatorname{Re}_\omega = \omega R_0^2 / \nu$, $V_0 = \omega R_0$, $\Omega_z = V_\varphi / r$, $Ha = B_0 R_0 \sqrt{\sigma / \rho\nu}$, $\delta_z = Z_0(Fo) / R_0$, $Fo = at / R_0^2$, a - temperature conductivity, t - time, σ, ρ, ν - electroconductivity, density and kinematic viscosity, $K_a = 1 - th\delta_z / \delta_z$ - reduction factor [5], taking into account the magnetic field weakening, and $C_0 = 0.0487$. Should be noted that Ha and Re_ω criteria and their combinations such as magnetic Taylor number [6] are defining for rotating MHD flows, including determination the point of transition to the turbulent regime.

In a directionally solidified ingot, the melt column height decreases when the ingot is solidified, and this is described in equation (1) by the relation of δ_z versus the Fourier criterion Fo.

Solidification proceeds much more slowly than the rearrangement of flow patterns, and therefore dimensionless time is used as a parameter. The dimensionless height of the melt column remains normalized to unity.

Boundary conditions for equation (1) are expressed as

$$V_\varphi\big|_{r=1} = 0, \quad V_\varphi\big|_{z=0} = 0, \ \frac{\partial V_\varphi}{\partial z}\Big|_{z=1} = 0. \tag{2}$$

The 2D secondary flow driven by rotation in the plane (r,z) is described by the azimuthal component ψ_φ of the hydrodynamic stream function $\vec{\psi}$ associated with the flow velocity via the relation $\vec{V} = rot\,\vec{\psi}$:

$$\Delta^2 \psi_\varphi - \lambda \Delta \psi_\varphi = -\frac{\operatorname{Re}_\omega}{\delta_z}\Omega_z \frac{\partial V_\varphi}{\partial z} = -\frac{\operatorname{Re}_\omega}{r\delta_z}\frac{\partial (rV_\varphi)}{\partial r}\frac{\partial V_\varphi}{\partial z}. \tag{3}$$

In the flow core $\Delta^2 \psi_\varphi << \lambda \Delta \psi_\varphi$, and this term can be neglected in the first approximation:

$$\Delta \psi_\varphi = \frac{\operatorname{Re}_\omega}{\lambda \delta_z r}\frac{\partial (rV_\varphi)}{\partial r}\frac{\partial V_\varphi}{\partial z}. \tag{4}$$

Boundary conditions for equation (4) take the form

$$\psi_\varphi\big|_{r=0,1} = 0, \quad \psi_\varphi\big|_{z=0,1} = 0. \tag{5}$$

For problem (1) – (2) we seek a solution using Galerkin's method in the form

$$V_\varphi = \sum_{k=1}^{\infty} N_k (1 + th\chi_k sh\chi_k z - ch\chi_k z) J_1(\gamma_k r), \tag{6}$$

where $N_k = 2Ha^2 \delta_z (Fo) K_a / \chi_k^2 \gamma_k J_2(\gamma_k)$, γ_k - roots of the equation $J_1(\gamma_k) = 0$, $\chi_k = \sqrt{\gamma_k^2 + \beta^2}$, $\beta^2 = \lambda + Ha^2 K_a$.

For problem (4) – (5) we seek a solution using Galerkin's method in the form

$$\psi_\varphi = \sum_{n=1,m=0}^{\infty} H_{nm} J_1(\gamma_n r) \sin(m + 1/2)\pi z, \tag{7}$$

where $H_{nm} = \frac{4 \operatorname{Re}_\omega I_{1nm}}{\lambda \delta_z [\gamma_n^2 + (m+1)^2 \pi^2] J_2^2(\gamma_n)}$, $I_{1nm} = \int_0^1 \int_0^1 \frac{\partial (rV_\varphi)}{\partial r}\frac{\partial V_\varphi}{\partial z} J_1(\gamma_n r) \sin(m + 1/2)\pi z \, dr\, dz$,

γ_n - roots of equation $J_1(\gamma_n) = 0$, and derivatives under the integrals are calculated from solution (6).

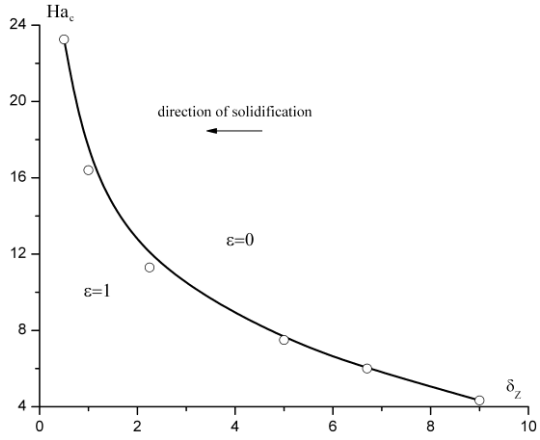

Fig. 2: Dependence of the critical values of the Hartmann number on δ_z. The curve divides the region into two domains with different flow regimes [4]: transitional ($\varepsilon = 1$) and turbulent ($\varepsilon = 0$). Three lower points – experimental data obtained from the test with pure tin, and three upper points – calculated data.

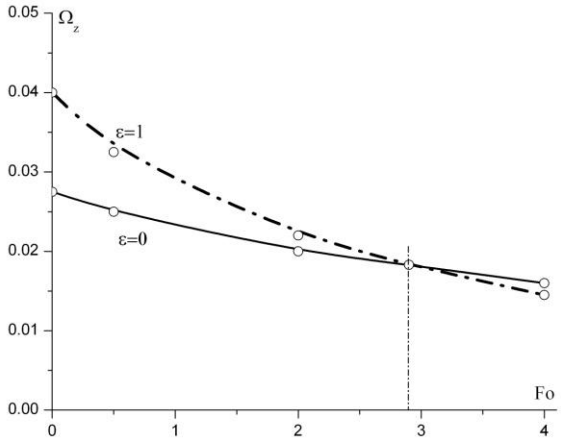

Fig. 3: Dimensionless angular velocity of rotation of the melt as a function of the Fourier criterion for two different values of the structural parameter ε [4] and determination of the point of transition from the turbulent flow regime ($\varepsilon = 0$) to the transitional non-laminar ($\varepsilon = 1$) flow regime; $Ha = 16.9$, $\mathrm{Re}_\omega = 5.6 \cdot 10^6$.

Analysis of results

Our study provides some estimates obtained during theoretical and experimental investigations. These findings make possible establishing a semi-empirical relation between the intensity and structure of the melt flow driven by RMF and the thermal characteristics of the flow near the crystallization front [1]. The flow regime is evaluated for different MHD-parameters, issues concerning the flow stability are examined (Figs. 2 and 3), and the thickness of the hydrodynamic boundary layer δ_h in the vicinity of the crystallization front is assessed (Fig. 4) from experimental data for commercially pure molten tin.

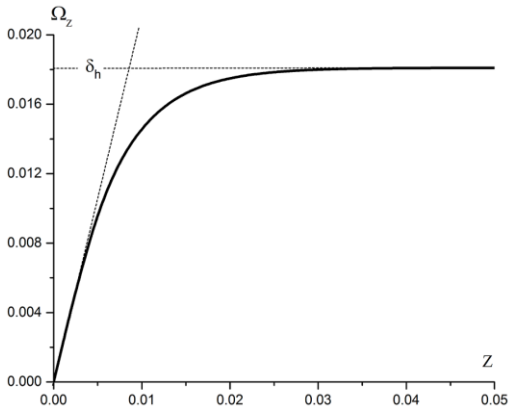

Fig. 4: Estimation of the thickness of the hydrodynamic boundary layer δ_h above the solidification front. Changes in the dimensionless angular velocity of rotation of the melt Ω_z along a normal to the crystallization front, $Ha = 11.2$.

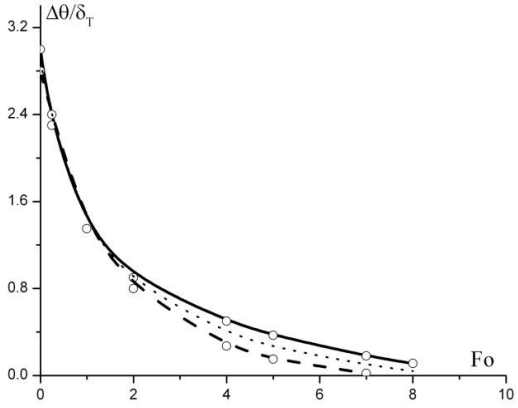

Fig. 5: Dimensionless temperature gradient in the thermal boundary layer as a function of the Fourier criterion, $Ha = 11.28 < Ha_{cr}$: dashed curve – along the z - axis of the mold, solid curve – 30 mm to the axis; dotted curve – mean values.

The experimental curves shown in Fig. 5 are characterized by a decrease in the dimensionless heat flow during solidification of the melt stirred in RMF for the Hartmann number Ha = 11.28, which is typical of the transitional regime near the point of transition to the turbulent flow realized at the critical Hartmann number Ha_{cr}. The averaged (dotted) curve is approximated well by the formula $\Delta\theta / \delta_T = 2.8 \cdot e^{-0.5Fo}$. Here, $\Delta\theta = (T_b - T_c)/(T_w - T_c)$;

T_b - temperature of the external edge of the boundary layer; $T_w = 370^0 C$ - temperature of the crucible wall; $T_c = 232^o C$ - tin solidification temperature; $\theta = (T_w - T)/(T_w - T_c)$; $Fo = 10.3 \cdot 10^{-3} t$ (t in seconds); δ_T - measured at the bottom of the mold.

The character of changes in the heat flow within the value interval $0 < Fo \le 0.5$ is attributed to heat extraction; further reduction in the heat flow is likely due to the formation of an air gap between the ingot and the bottom of the crucible and due to heating of the crucible sidewall.

Because of the non-dimensional form of obtained results, it is supposed to use them in the study of the RMF impact on the macrostructure of various pure metals. Fig. 6 presents photographs illustrating differences in the macrostructures of commercially pure aluminium ingots obtained during directional solidification without MHD-effects (a), and in the presence of azimuthal MHD stirring under RMF impact (b), (c). The Ha and Re_ω criteria values in experiments were set near critical, so that the rotating flow regimes were close to the transition point.

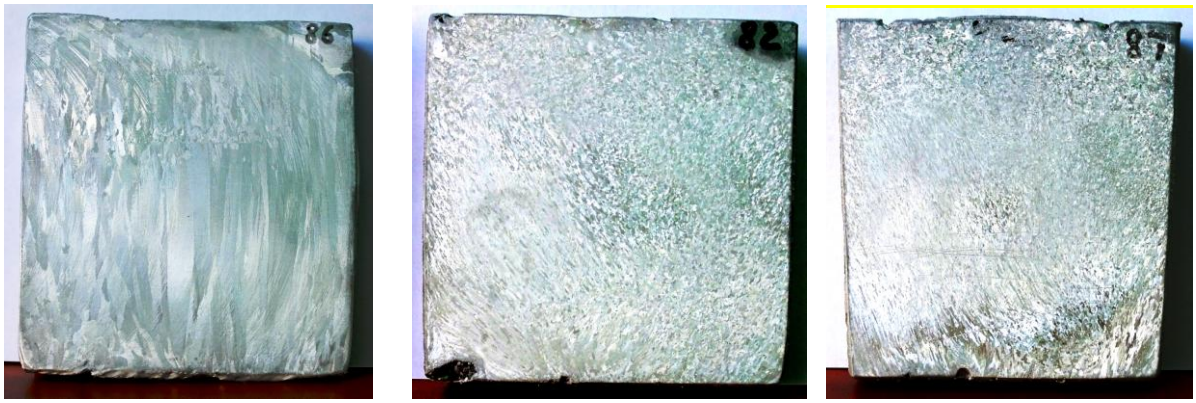

a) b) c)

Fig.6: Structure of the aluminium ingot during the directional solidification process. The capacity of the heater used to heat crucible walls – 1200 W. Water discharge rate and temperature – 40cm^3/sec and 12^{0}C, respectively: a) without MHD stirring, and with azimuthal stirring by RMF inductor at: b) $Ha = 10.5, \mathrm{Re}_\omega = 1 \cdot 10^6$; c) $Ha = 15.6, \mathrm{Re}_\omega = 1 \cdot 10^6$.

Further analysis of macro- and microstructure of samples together with the parameters of a rotating magnetic field and the parameters of temperature and heat boundary layers should provide a potentiality for a priori estimates for structures of interest.

Conclusions

- Using theoretical and experimental data, we have established some definite relations between the parameters that characterize the MHD effects on liquid metal and the parameters of boundary layers occurred at the crystallization front.
- We have analyzed a relation between the critical MHD parameters determining a structural transition between the turbulent and non-turbulent regimes of the melt flow and the peculiarities of changes of thermal boundary layers parameters.
- Summing up, the results obtained from the analysis of macro- and microstructure of samples subjected to MHD effects should be defined more exactly and will be reported in our presentation.

References

[1] A. Kapusta, B. Mikhailovich, S. Khripchenko, I. Kolesnichenko (2015), Magnetohydrodynamics 51 (3), in press
[2] S. Yu. Khripchenko, L.V. Nikulin, V. M. Dolgikh, S. A. Denisov (2014), Non-Ferrous Metals 6, 82-86
[3] S. Denisov, V. Dolgikh , S. Khripchenko, I. Kolesnichenko , L. Nikulin (2014), Magnetohydrodynamics 50 (4), 249-265
[4] E. Golbraikh, A. Kapusta, B. Mikhailovich (2007), Magnetohydrodynamics 43 (1), 35-44
[5] V. A. Teearu (1965), Coll. Articles NISETI, Energia, Moscow – Leningrad, 91-101
[6] I. Grants, G. Gerbeth (2001), Journal of Fluid Mechanics 431, 407-426